

Characterization of Micromachined Waveguide Hybrids at 350 and 650 GHz

Axel Murk, Stephan Biber, Thomas Tils, Patrick Pütz, Lorenz-Peter Schmidt and Niklaus Kämpfer

Abstract—We present measurement results of two different hybrid couplers at submillimeter wavelengths. The devices under test were a 650 GHz coupler, which has been micromachined in Silicon by deep reactive ion etching, and two versions of a 345 GHz coupler machined out of brass. In order to determine the amplitude and phase balance of the coupling section the differences between the connecting waveguides have to be taken into account. We corrected the measurements under the assumption that the coupling section itself is fully symmetrical, which results in a good matching between the measured and the simulated performance.

I. INTRODUCTION

Waveguide hybrids are a prerequisite for balanced and sideband separating mixers. At lower frequencies they are available off-the-shelf from various suppliers, but above 100 GHz they are increasingly difficult to manufacture because of the tighter mechanical tolerances. Currently several research institutes are developing hybrids for submillimeter wavelengths, mostly for radio astronomical applications [1], [2]. Measurements have been reported so far for 70–110 GHz [3] and 257–370 GHz [4].

A 90° waveguide hybrid is a directional 4-port device that distributes a signal at its input port 1 equally and with a well defined phase shift of 90° between the two output ports 3 and 4. The second input port 2 is fully isolated from port 1 and has the same symmetrical coupling to ports 4 and 3. Figure 1 shows a typical layout of a branchline coupler and electrical field simulations with the software package CST Microwave Studio.

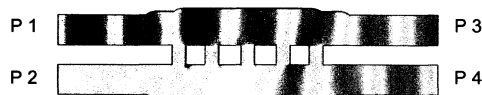


Fig. 1. Layout of a 90° branchline coupler. The colors represent the simulated electrical field when a signal is injected at port 1.

This work was supported by the Swiss National Science Foundation, grant 200020-100167, by the Deutsche Forschungsgemeinschaft, grant SFB 494, and by the European Union, grant FP6-Radionet. P. Pütz would like to thank C. Groppi, University of Arizona, for milling one of the 345 GHz couplers.

A. Murk and N. Kämpfer are with the Institute of Applied Physics, University of Bern, Switzerland (axel.murk@mw.iap.unibe.ch).

T. Tils is with the Kölner Observatorium für Submillimeter Astronomie, University of Köln, Germany.

P. Pütz is with the Steward Observatory Radioastronomy Laboratory, University of Arizona, USA, and also with the Kölner Observatorium für Submillimeter Astronomie, Germany.

S. Biber and L.P. Schmidt are with the Lehrstuhl für Hochfrequenztechnik, University of Erlangen-Nürnberg, Germany. S. Biber is now with Siemens Corporate Technology, Erlangen, Germany.

II. COUPLER DESIGN

The following two waveguide hybrids have been realized:

Coupler A from the Kölner Observatorium für Submillimeter Astronomie (KOSMA) has a center frequency of 345 GHz and was micromachined in brass on a high speed *Deckel FP-2* milling machine [5]. A second version of this coupler was manufactured at Steward Observatory Radioastronomy Laboratory (SORAL) using a more accurate *Kern MMP* milling machine.

Coupler B from the University of Erlangen-Nürnberg has a center frequency of 650 GHz and was micromachined in Silicon by photolithography, Deep Reactive Ion Etching (DRIE) and gold plating of the surfaces [6].

Both couplers are assembled from two symmetrical split-block halves that are cutting the waveguide in the E-plane. Figure 2 shows the 345 GHz brass coupler A, and Figure 3 the overall dimensions and electron microscope images of the etched Silicon coupler B. To have sufficient space for the input and output flanges both test devices include S-shaped waveguide sections that are much longer than the actual coupling regions. The phase errors in these waveguides and differences between their flanges have a significant effect on the measurement results.

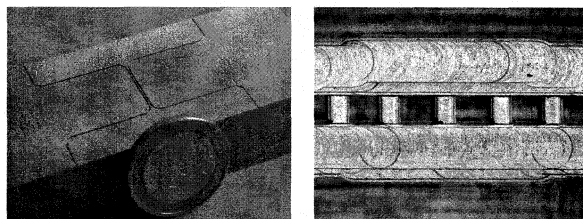


Fig. 2. Coupler A for 345 GHz: Split-block half milled out of brass (left) and its branchline section (right).

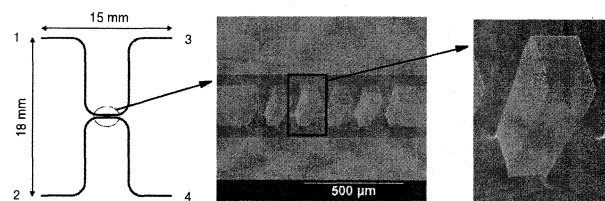


Fig. 3. Coupler B for 650 GHz etched out of a Silicon wafer.

III. MEASUREMENT SETUP

The transmission characteristics of the couplers were measured with an *AB-Millimetre* vector network analyzer. Its submillimeter wave source module, which consists of a phase-locked W-band Gunn oscillator and a multiplier, was connected to port 1 or 2 of the coupler through a 220 GHz or 550 GHz highpass filter and appropriate waveguide transitions. For the measurements of the 650 GHz device flexible dielectric waveguides with a high phase stability were used to simplify the change between different ports [7]. The detector was a simple harmonic mixer for the measurements around 345 GHz, and another harmonic mixer pumped by a second Gunn oscillator for those around 650 GHz. Again custom made waveguide transitions were used to connect the detector to the device under test.

The two unused ports of the coupler have to be terminated by a matched load during the measurements. Since waveguide loads were not available at these frequencies we used horn antennas that were pointing on a submillimeter wave absorber. For the 345 GHz coupler electroformed smooth-walled horn antennas with a spline profile were used [8], for the 650 GHz coupler octagonal horns etched in Silicon [9]. The mismatch and loss at the flanges was generally worse for the 650 GHz device because of the difficulties to machine them accurately in Silicon. For that reason these measurements are more affected by reflections and standing waves.

The maximum span of a frequency sweep was only about 1.5 GHz because of the limited electrical tuning range of the Gunn oscillator. For that reason each test sequence of all possible port combinations S_{ij} had to be repeated after tuning the vector analyzer to a new center frequency. A dedicated waveguide calibration kit was not available for these frequency bands, and only a simple through measurement (labeled *Ref*) without the coupler was made after each tuning step. Since the complete test procedure is very time consuming the couplers were tested with a limited number of frequency sweeps, and not continuously over their full bandwidth.

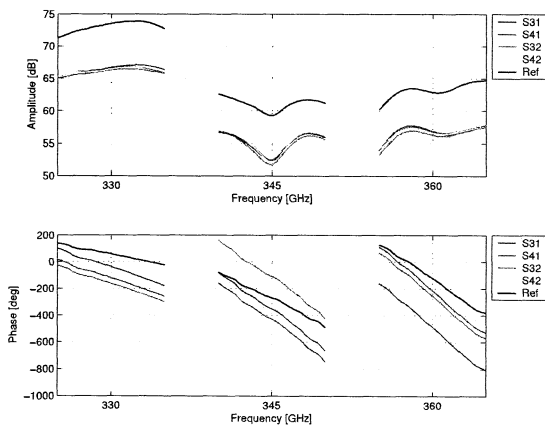


Fig. 4. Raw data of coupler A.

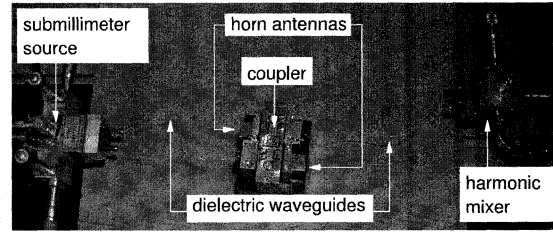


Fig. 5. Test setup for the 650 GHz coupler. The absorber terminations in front of the horn antennas are not shown in this picture.

IV. RESULTS

Figures 4 and 6 show the raw data of the measurement series. Amplitude and phase depend strongly on the sensitivity and the tuning of the detector and the source. In these and the following figures the span of the frequency sweeps has been expanded for clarity and the frequency axis is not to scale.

The measurements are also affected by standing waves in the test setup. The standing wave pattern is very similar for the various S_{ij} measurements because they involve the same number of waveguide interfaces and similar electrical lengths, but it is completely different for the *Ref* measurement. Since we are mostly interested in the amplitude and phase balance between the S_{31} and S_{41} , each series of frequency sweeps is calibrated using the complex S_{31} data as reference. In addition the data is scaled to obtain a mean amplitude of 0 dB for the through measurement *Ref*:

$$S_{ij\text{calibrated}} = \frac{S_{ij}}{S_{31}} \cdot \text{mean} \left(\left| \frac{S_{31}}{Ref} \right| \right).$$

Figures 7 and 9 show the calibrated data. The S_{31} measurements appear now with a constant amplitude and zero degree phase because they were used as reference plane. The phase slope of *Ref* is given by the electrical length of the coupler. The *Ref* measurements were repeated after each test series to check the repeatability of the measurements. A significant drift occurred only in the frequency sweeps around 675 and 700 GHz, and the results at these frequencies will be less

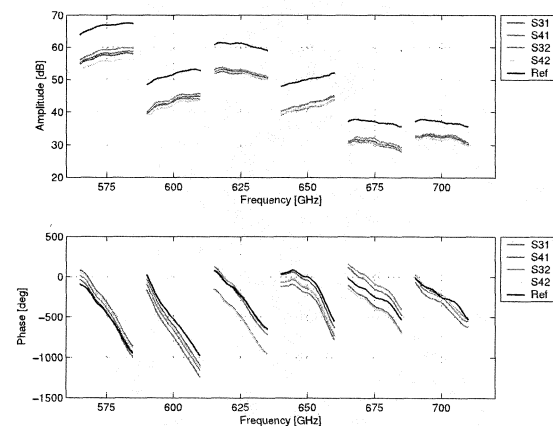


Fig. 6. Raw data of coupler B

reliable. The strong ripple on the *Ref* phase at 700 GHz also indicates that this measurement was more affected by standing waves than the others.

Another important parameter of a coupler is the isolation S_{12} and S_{34} . For both couplers values between -20 and -25 dB have been measured. Model simulations predict similar values, but some discrepancies exist because of the mismatch at the terminated ports.

V. ERROR CORRECTION

The calibrated data in Figures 7 and 9 differ significantly from the expected behavior. The design of both couplers has been optimized to be close to an ideal waveguide hybrid with $S_{41} = S_{31} \cdot \exp(i\frac{\pi}{2})$ and $S_{42} = S_{32} \cdot \exp(i\frac{\pi}{2})$. In addition the symmetrical layout should result in $S_{31} = S_{42}$ and $S_{41} = S_{32}$, which is not the case in the calibrated data.

A significant part of the observed unbalance is not a true characteristic of the branchline section of the coupler, but a difference in its electrically long waveguide connections and its flanges. These errors can be corrected under the assumption that the coupler itself is symmetric. Figure 8 shows a simple error model of the test setup. The coupling section C is connected with the four test ports through transmission lines that are not identical. Since S_{31} is used as reference plane ports 1 and 3 are free of errors, while port 2 and 4 have an additional complex gain e_2 and e_4 .

The measurements S_{ij} are related to the true values S_{ij}' as:

$$\begin{aligned} S_{31} &= S_{31}' && \text{reference plane} \\ S_{41} &= S_{41}' \cdot e_2 \\ S_{32} &= S_{32}' \cdot e_4 \\ S_{42} &= S_{42}' \cdot e_2 \cdot e_4. \end{aligned}$$

If we assume that the coupling section C is symmetric, then $S_{31}' = S_{42}'$ and $S_{32}' = S_{41}'$. In this case the error terms can be calculated with:

$$e_2 = \sqrt{\frac{S_{42} \cdot S_{41}}{S_{31} \cdot S_{32}}} \quad e_4 = \sqrt{\frac{S_{42} \cdot S_{32}}{S_{31} \cdot S_{41}}}$$

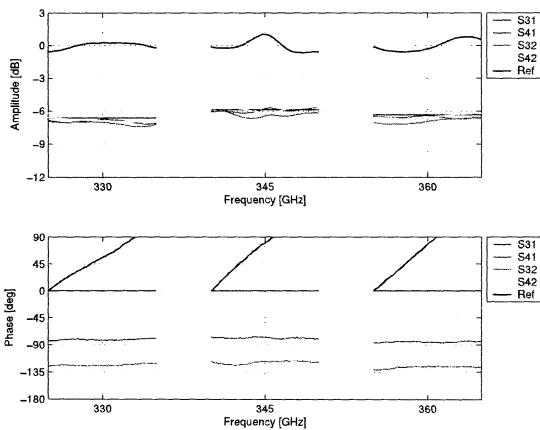


Fig. 7. Calibrated data of coupler A.

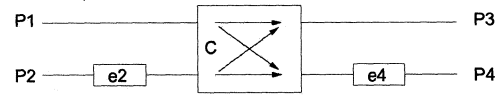


Fig. 8. Model for the error correction: if the coupler element C is assumed to be symmetric, then the errors e_2 and e_4 of ports 1 and 2 can be calculated from the four transmission measurements.

Figures 10 and 11 show the corrected results. The mean values of amplitude and phase are now equal for symmetrical signal paths according to the assumptions that were made, and for that reason only the S_{31} and S_{41} values are shown. The power is now distributed almost equally and with a phase shift close to 90° between the two output ports, at least for the designed band center of the coupler. This shows that the design goals of the couplers could be reproduced within the accuracy of our measurement setup. Two versions of the 345 GHz coupler have been tested. Device #2, which has been produced with the better milling machine, has a flatter amplitude and phase response over the frequency band. The measurements at 675 and 700 GHz remain questionable because of the observed drift and standing waves problems.

The absolute amplitude of the corrected data is significantly smaller than the -3 dB of an ideal coupler because of the losses in the waveguides and at the flanges. For the 345 GHz device the observed values below -6 dB correspond very well with CST simulations of the complete structure when the ohmic loss of brass is taken into account in the model. This losses could be significantly reduced by gold plating or machining in a low-loss material, e.g. Tellurium-Copper. For the 650 GHz device the losses differ by typically 1 to 2 dB from model estimates, most likely because of the imperfections of the waveguide flanges and of the etching process.

VI. DISCUSSION

There is some concern about the validity of the proposed correction scheme. It could be questioned whether the 90° phase difference of the corrected data is an implicit result of our assumptions because every matched ($S_{ii} = 0$), lossless

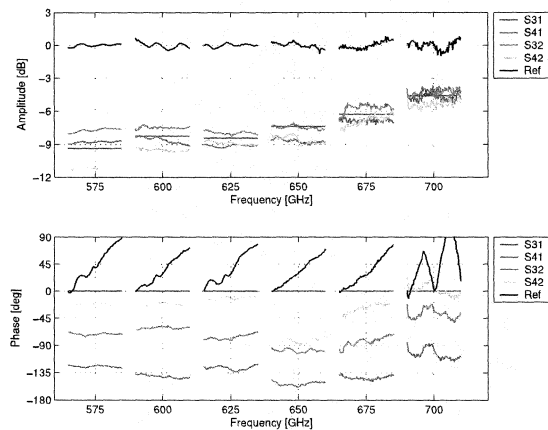


Fig. 9. Calibrated data of coupler B.

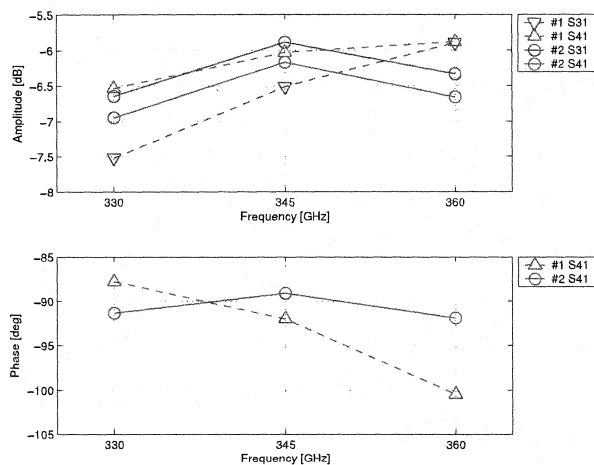


Fig. 10. Corrected data of coupler A (#1: KOSMA, #2: SORAL).

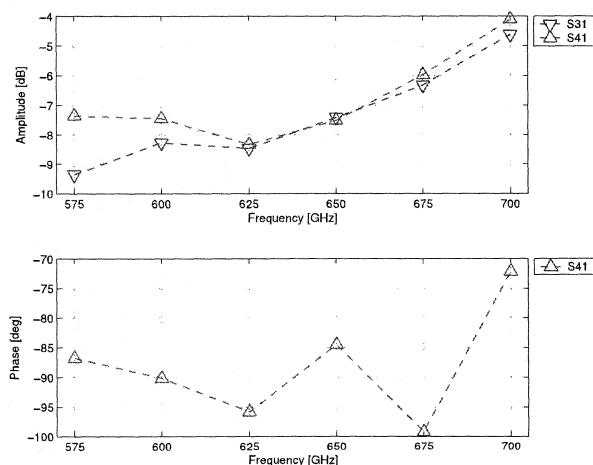


Fig. 11. Corrected data of coupler B.

and double-symmetric 4-port device produces exactly this phase shift between its output ports. Our correction scheme, however, includes only the assumption of a single symmetry plane in the coupling section. This is justified by the symmetric layout of the coupler, and it is still valid for the most likely manufacturing errors, e.g. when the two splitblocks are not perfectly aligned or when the width of the branchlines is incorrect. We tested with CST simulations that only large asymmetric machining errors will break this symmetry. In this case the correction will obviously lead to wrong results, but not automatically to a 90° phase shift.

Multiple reflections are not corrected with the described method, but this problem can not be resolved without further calibration standards, better flanges or much wider instantaneous frequency sweeps. Especially the measurements of the 650 GHz device are affected by standing waves. Another possible error source are phase shifts in the cables with the reference signals of the network analyzer when the source or detector are swapped between different ports. For that reason we used high quality cables and tried to move them as little as possible during a test series. The reproducibility of the *Ref2* measurement, the phase difference of the corrected data close to 90° and the consistency of the correction factors *e* at different frequencies indicate that these errors were only a couple of degrees in most cases. For the measurements of the 650 GHz coupler the source and detector remained fixed on the test bench, and only the dielectric waveguides had to be swapped between the ports. The phase stability of these waveguides had been tested before and proved to be sufficient for our measurements.

The reason for the necessary corrections has been investigated in more detail for two 345 GHz couplers. The amplitudes of *e1* and *e2* are within ± 0.2 dB with a variation of about ± 0.1 dB between different frequency sweeps. The phases are between $+10^\circ$ and -30° and change only little with frequency, which translates to a pathlength difference of up to 0.25 mm. Because it is unlikely that the mechanical length

of the waveguide sections differs that much we measured their width and height under a microscope at different locations in the split-block. It turned out that the milling tolerances cause a certain variability of the propagation constant, and because of the large total length of the waveguides this can add up to similar phase errors as the observed ones.

The length of the waveguide sections will be significantly shorter and flanges can be avoided by integrating the coupler into the mixer block of a sideband separating receiver. In this case it can be expected from our measurements that the power splitting and phase difference will be close to the design goal of -3 dB and 90° .

REFERENCES

- [1] J. W. Kooi, A. Kovács, B. Bumble, G. Chattopadhyay, M. L. Edgar, S. Kaye, R. LeDuc, J. Zmuidzinas, and T. G. Phillips, "Heterodyne instrumentation upgrade at the Caltech Submillimeter Observatory," in *Proceedings of SPIE: Astronomical Telescopes and Instrumentation*, vol. 5498-40, pp. 332-348, June 2004.
- [2] S. Claude, C. Cunningham, A. Kerr, and S. Pan, "Design of a sideband-separating balanced SIS mixer based on waveguide hybrids," in *ALMA Memo*, no. 316, Sept. 2000.
- [3] S. Srikanth and A. R. Kerr, "Waveguide quadrature hybrids for ALMA receivers," in *ALMA Memo*, no. 343, Jan. 2001.
- [4] S. Claude, "Sideband-separating SIS mixer for ALMA band 7, 275-370 GHz," in *ALMA Memo*, no. 357, Mar. 2001.
- [5] T. Tils, *Design and 3-D Electromagnetic Modeling of Terahertz Waveguide Mixers and Components*. Phd thesis, Universität zu Köln, 2006.
- [6] S. Biber, *Mikrostrukturierte Terahertz-Bauelemente auf Silizium-Basis*. Phd thesis, Technische Fakultät der Universität Erlangen-Nürnberg, 2005. Available online at <http://www.opus.ub.uni-erlangen.de>.
- [7] A. Hofmann, E. Hörster, J. Weinzierl, L.-P. Schmidt, and H. Brand, "Flexible low-loss dielectric waveguides for THz frequencies with transitions to metal waveguides," in *33rd European Microwave Conference*, pp. 955-958, 2003.
- [8] T. Lüthi, D. Rabanus, U. Graf, C. Granet, and A. Murk, "A new multi-beam receiver for KOSMA with scalable fully reflective focal plane array optics," in *16th International Symposium on Space Terahertz Technology*, May 2005.
- [9] S. Biber, A. Murk, L. P. Schmidt, and N. Kämpfer, "Design and measurement of a 600 GHz micromachined horn antenna manufactured by combined DRIE and KOH-etching of silicon," in *16th International Symposium on Space Terahertz Technology*, May 2005.